Journal of Sound and Vibration 325 (2009) 499–506

Contents lists available at ScienceDirect

Journal of Sound and Vibration

journal homepage: www.elsevier.com/locate/jsvi

Rapid Communication

Forced vibrations of a torsional oscillator with Coulomb friction under a periodically varying normal load

Chengwu Duan, Rajendra Singh *

Acoustics and Dynamics Laboratory, Department of Mechanical Engineering, The Ohio State University, Columbus, OH 43210, USA

ARTICLE INFO

Article history:
Received 13 January 2009
Received in revised form
2 April 2009
Accepted 2 April 2009
Handling Editor: L.N. Virgin
Available online 2 May 2009

ABSTRACT

The forced vibration response of a single degree of freedom torsional system with Coulomb friction, under a periodically varying normal load, is studied. First, an enhanced multi-term harmonic balance method is developed to calculate nonlinear responses directly in frequency domain; this should be in general applicable to periodically varying nonlinear systems. Second, a pulse width modulated normal load is approximated by a truncated Fourier series with a reasonable number of harmonic components and utilized for case studies. Finally, the effects of duty ratio on nonlinear frequency responses are examined.

1. Introduction

There is a large body of literature on time-invariant friction dynamics [1–4], starting from Den Hartog who studied frequency response by assuming that the friction interface experiences no more than two stops in one cycle [1]. In contrast, the time-varying friction problem, say when the normal load varies with time, is relatively less studied. In clutches, brakes and other driveline systems, the normal load (or torque) usually varies with time; such variations are usually caused by surface undulations or changes in frictional contact regimes. For instance, changes in the brake rotor thickness lead to a corresponding variation in the normal load in brake judder problems [5]. Recently, we numerically examined the influence of time-varying friction in a two degree of freedom torsional system, in which the dry friction acts as a power transmission path with application to an automotive driveline problem [6]. Badertscher et al. experimentally studied the response of a single degree of freedom system under normal dither loads, with application to brake squeal control [7]. However, prior formulations are limited to sinusoidally varying normal loads. This motivates us to examine the forced response of an oscillator with dry friction under periodically varying normal load. Further, since previous frequency domain solutions are limited to nonlinear time-invariant systems [8–11], we propose an enhanced semi-analytical multi-term harmonic balance method (MHBM) that could be employed to construct solutions to nonlinear time-varying system problems [12].

2. Problem formulation

Consider a single degree of freedom torsional system with both dry friction and viscous damping elements (in parallel), as shown in Fig. 1. The nonlinear friction torque is a function of periodically varying normal load $N(\tau)$. The governing

* Corresponding author.
E-mail address: singh.3@osu.edu (R. Singh).

0022-460X/$ - see front matter © 2009 Elsevier Ltd. All rights reserved.
doi:10.1016/j.jsv.2009.04.003

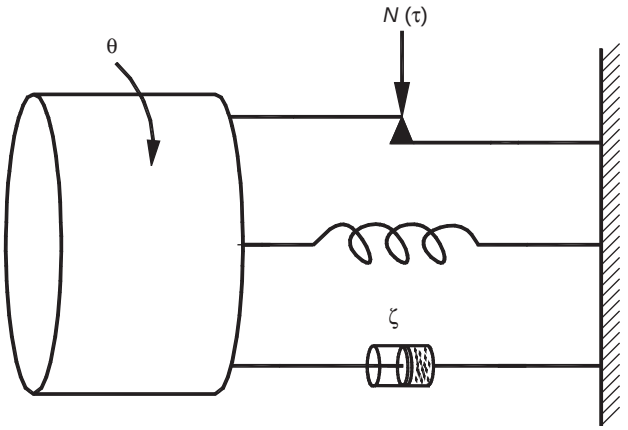

Fig. 1. Single degree of freedom torsional system with both dry friction (under periodically varying normal load $N(\tau)$) and viscous damping elements.

equation (in the dimensionless form) is as follows where $(.)' = \mathrm{d}(.)/\mathrm{d}\tau$ and $(.)'' = \mathrm{d}^2(.)/\mathrm{d}\tau^2$:

$$\theta'' + 2\zeta\theta' + \theta + T_f(\theta', \tau) = T_p \sin(\Omega\tau) \tag{1}$$

where ς is the viscous damping ratio, θ is the angular displacement and T_p is the amplitude of externally applied harmonic torque at Ω. The nonlinear time-varying friction torque is given by a product of speed-dependent friction coefficient $\mu(\theta')$, effective arm of moment r and $N(\tau)$ as:

$$T_f(\theta', \tau) = r\mu(\theta')N(\tau) \tag{2}$$

Assume that $N(\tau)$ is periodic with fundamental frequency Ω/κ where κ is an integer of sub-harmonic index and Ω is the frequency of external torque. Also the classical Coulomb friction is assumed with μ_s as static (or kinetic) friction coefficient. Thus, represent $N(\tau)$ by Fourier series as:

$$N(\tau) = N_0 + \sum_{n=1}\left(N_{2n-1}\sin\left(\frac{n}{\kappa}\Omega\tau\right) + N_{2n}\cos\left(\frac{n}{\kappa}\Omega\tau\right)\right), \tag{3a}$$

$$\mu(\theta') = \begin{cases} \mu_s & |\theta'| > 0 \\ [-\mu_s \;\; \mu_s] & |\theta'| = 0 \end{cases}. \tag{3b}$$

The primary objective of this communication is to study the nonlinear frequency response of Eq. (1). An enhanced multi-term harmonic balance method is proposed to directly calculate the nonlinear forced response in frequency domain. The feasibility of the proposed semi-analytical method is demonstrated and validated with Runge–Kutta numerical integration. A pulse width modulated $N(t)$ is then considered and the effects of pulse duty ratio on nonlinear responses are briefly studied.

3. Enhanced harmonic balance method for nonlinear time-varying systems

The multi-term harmonic balance method has previously been applied to mainly construct periodic solutions to nonlinear time-invariant systems [8–11]. Thus, we re-formulate it for application to a nonlinear time-varying system as defined by Eq. (1) and determine the periodic response of $\theta(\tau)$. A generic formulation for solving the nonlinear time-varying system is first illustrated. Essentially, the multi-term harmonic balance method constructs approximate periodic responses that are represented by a truncated Fourier series, as shown below, where N_h is the harmonic order and υ is the sub-harmonic index. For the sake of illustration, the nonlinear term in Eq. (1) is further generalized in a manner similar to separation of variables, $T_f(\theta, \dot{\theta}, t) = u(\theta)v(\theta')q(\tau)$, i.e. the nonlinear friction torque is a product of three functions of θ, θ' and τ, respectively.

$$\theta(\tau) = a_0 + \sum_{n=1}^{N_h\upsilon}\left(a_{2n-1}\sin\left(\frac{n}{\upsilon}\Omega\tau\right) + a_{2n}\cos\left(\frac{n}{\upsilon}\Omega\tau\right)\right) \overset{\text{discretize}}{\longrightarrow} \boldsymbol{\theta} = \boldsymbol{\Delta}\mathbf{a}, \tag{4a}$$

$$T_f = b_0 + \sum_{n=1}^{N_h\upsilon}\left(b_{2n-1}\sin\left(\frac{n}{\upsilon}\Omega\tau\right) + b_{2n}\cos\left(\frac{n}{\upsilon}\Omega\tau\right)\right) \overset{\text{discretize}}{\longrightarrow} \mathbf{T_f} = \boldsymbol{\Delta}\mathbf{b}. \tag{4b}$$

Here, $\mathbf{\Delta}$ is the discrete inverse Fourier transform operator:

$$\mathbf{\Delta} = \begin{bmatrix} 1 & \sin\left(\frac{n}{\upsilon}\Omega\tau_0\right) & \cos\left(\frac{n}{\upsilon}\Omega\tau_0\right) & \cdots & \cos\left(\frac{N_h\upsilon}{\upsilon}\Omega\tau_0\right) \\ \vdots & \vdots & \vdots & \vdots & \vdots \\ 1 & \sin\left(\frac{n}{\upsilon}\Omega\tau_{K-1}\right) & \cos\left(\frac{n}{\upsilon}\Omega\tau_{K-1}\right) & \cdots & \cos\left(\frac{N_h\upsilon}{\upsilon}\Omega\tau_{K-1}\right) \end{bmatrix}. \tag{5}$$

And $\mathbf{a} = [a_0\ \ a_1 \ldots a_{2N_h\upsilon}]^{\mathrm{T}}$, $\mathbf{b} = [b_0\ \ b_1 \ldots b_{2N_h\upsilon}]^{\mathrm{T}}$. Next, Eq. (1) is solved by transforming it into an algebraic problem and then the harmonic coefficients between excitation (with coefficient T_P and denoted as $\mathbf{p}$ in vector format) and responses are matched. Next, the numerical iteration process is employed to minimize the residue $\mathbf{R}$ where $\mathbf{D}$ is a differentiator and $\mathbf{b} = \mathbf{\Delta}^{+}\mathbf{T_f}$, where $\mathbf{\Delta}^{+}$ represents a pseudo inverse $(\mathbf{\Delta^T\Delta})^{-1}\mathbf{\Delta^T}$; for application to nonlinear time-invariant systems, refer to our previous paper [11].

$$\mathbf{D} = \begin{bmatrix} 0 & & & & \\ & \ddots & & & \\ & & \begin{bmatrix} 0 & -n/\upsilon \\ n/\upsilon & 0 \end{bmatrix} & & \\ & & & \ddots & \end{bmatrix}, \tag{6a}$$

$$\mathbf{R} = \Omega^2\mathbf{D}^2\mathbf{a} + 2\zeta\Omega\mathbf{D}\mathbf{a} + \mathbf{a} + \mathbf{b} - \mathbf{p}. \tag{6b}$$

To ensure the minimization process following the deepest descent, define the Jacobian ($\mathbf{J}$) matrix as:

$$\mathbf{J} = \frac{\partial\mathbf{R}}{\partial\mathbf{a}} = \Omega^2\mathbf{D}^2 + 2\zeta\Omega\mathbf{D} + \frac{\partial\mathbf{a}}{\partial\mathbf{a}} + \frac{\partial\mathbf{b}}{\partial\mathbf{a}}. \tag{7}$$

Since θ is periodic, $u(\theta)$ and $v(\theta')$ are also periodic. In addition, the periodic $q(\tau)$ can be expressed as $\mathbf{q}(\tau) = \mathbf{\Delta c}$, since it is independent from θ and θ' and $\mathbf{c}$ is usually a known vector. Consequently, the following $\partial\mathbf{b}/\partial\mathbf{a}$ expression holds,

$$\frac{\partial\mathbf{b}}{\partial\mathbf{a}} = \left(\frac{\partial\mathbf{b}}{\partial\mathbf{T_f}}\right)\left[\frac{\partial\mathbf{T_f}}{\partial\boldsymbol{\theta}}\frac{\partial\boldsymbol{\theta}}{\partial\mathbf{a}} + \frac{\partial\mathbf{T_f}}{\partial\boldsymbol{\theta}'}\frac{\partial\boldsymbol{\theta}'}{\partial\mathbf{a}}\right], \tag{8a}$$

$$\frac{\partial\mathbf{T_f}}{\partial\boldsymbol{\theta}} = \mathrm{diag}[\mathbf{v}(\theta')]\mathrm{diag}[\mathbf{q}(\tau)]\left[\frac{\partial\mathbf{u}(\theta)}{\partial\boldsymbol{\theta}}\right], \quad \frac{\partial\boldsymbol{\theta}}{\partial\mathbf{a}} = \mathbf{\Delta}, \tag{8b,c}$$

$$\frac{\partial\mathbf{T_f}}{\partial\boldsymbol{\theta}'} = \mathrm{diag}[\mathbf{u}(\theta)]\mathrm{diag}[\mathbf{q}(\tau)]\left[\frac{\partial\mathbf{v}(\theta')}{\partial\boldsymbol{\theta}'}\right], \quad \frac{\partial\boldsymbol{\theta}'}{\partial\mathbf{a}} = \Omega\mathbf{\Delta D}. \tag{8d,e}$$

Here diag[ ] is an operator to diagonalize one-dimensional vectors. Finally, the path following technique is used to calculate the turning points. The basic idea is to include $\partial\mathbf{R}/\partial\Omega$ as an independent vector and form an augmented $\mathbf{J}$.

$$\frac{\partial\mathbf{R}}{\partial\Omega} = 2\Omega\mathbf{D}^2 + 2\zeta\mathbf{D} + \frac{\partial\mathbf{b}}{\partial\Omega}, \tag{9a}$$

$$\frac{\partial\mathbf{b}}{\partial\Omega} = \frac{\partial\mathbf{b}}{\partial\mathbf{T_f}}\frac{\partial\mathbf{v}(\theta')}{\partial\boldsymbol{\theta}'}\frac{\partial\boldsymbol{\theta}'}{\partial\Omega}. \tag{9b}$$

To apply the above formulation to the problem at hand, one should simply replace $u(\theta)$ with an identity, $v(\theta')$ with $\mu(\theta')$ and $q(\tau)$ with $N(\tau)$.

To assess the feasibility of multi-term harmonic balance method, consider a periodically varying normal load $\mathbf{N}(\tau) = \mathbf{\Delta d}$ and $\mathbf{d} = [0.6\ \ 0.2\ \ 0.1\ \ 0.3\ \ -0.4]^{\mathrm{T}}$. Fig. 2 shows the nonlinear frequency responses of the time-varying system. Clearly, the responses of nonlinear time-invariant ($\mathbf{d} = [0.6\ \ 0\ \ 0\ \ 0\ \ 0]^{\mathrm{T}}$) and time-varying systems significantly differ. For the sake of validation, Eq. (1) is also numerically solved using Runge–Kutta algorithm [13]. As shown in Fig. 2, an excellent match between multi-term harmonic balance method and numerical integration solutions is evident over the entire frequency range of interest. Jump phenomena that are typically observed in nonlinear stiffness problems [14] do not occur here. This can be explained by the fact that dry friction is essentially a nonlinear damping element that does not change the effective stiffness of the system and thus the backbone curves do not bend or fold. Consequently, the path following technique is not necessary for this type of problem though it is widely used to calculate multi-valued solutions [15] by adaptively adjusting the frequency step. Accordingly, the frequency response maps (or contour plots) that require equal-spaced frequency points for a variation in the duty ratio (as presented in Section 5) are generated without employing the path following technique.

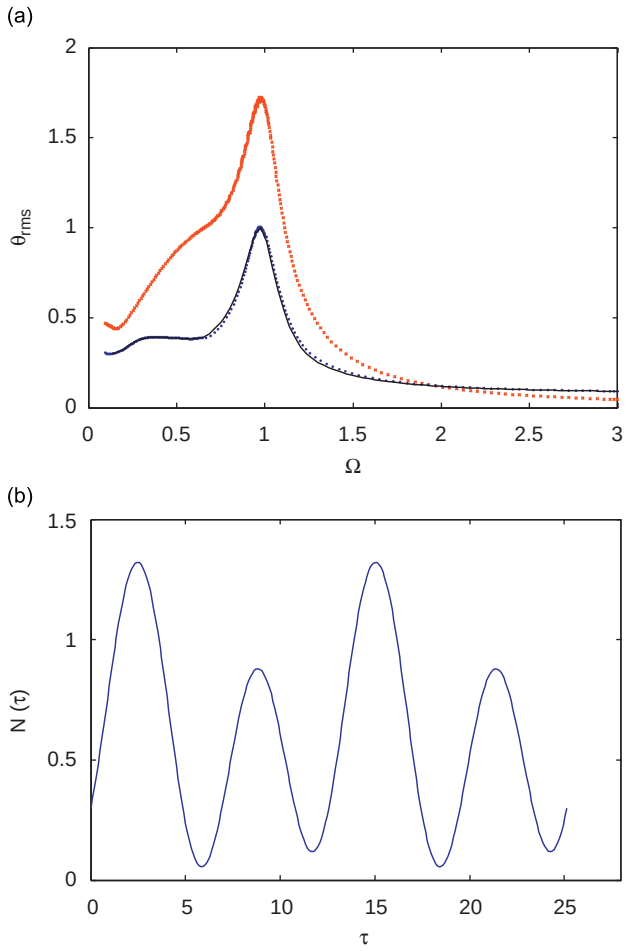

Fig. 2. Validation of the multi-term harmonic balance method (MHBM). (a) Comparison of nonlinear frequency responses between nonlinear time-varying and time-invariant systems corresponding to Eq (5). Key: × × ×, nonlinear time-invariant system using MHBM; ●●●, nonlinear time-varying system using MHBM; —, nonlinear time-varying system using numerical integration. (b) Periodically varying normal load at $\boldsymbol{\Omega} = 0.5$.

4. Pulse width modulated normal load

Next, we apply the enhance MHBM to a pulse-width modulated normal load as shown in Fig. 3. Note that $N(\tau)$ is semi-definite-positive and we do not consider separation between friction surfaces. In our study, we assume the pulse has the same period P (or frequency) as T_p for the sake of conciseness, i.e. $P = 2\pi/\Omega$. Taking into account the time delay $\tau_g \in [0P)$ between $N(\tau)$ and T_p and duty ratio $\alpha \in [0\ 1]$, the pulse can be further approximated by Fourier series, $N(\tau) = p_0 + \sum_{n=1} p_n \sin(n\Omega\tau) + q_n \cos(n\Omega\tau)$, with the following coefficients, where Q is the magnitude of the normal load.

$$p_0 = Q\alpha, \tag{10a}$$

$$p_n = \frac{-Q}{n\pi}[\cos(n\Omega\tau_g + 2n\pi\alpha) - \cos(n\Omega\tau_g)], \tag{10b}$$

$$q_n = \frac{Q}{n\pi}[\sin(n\Omega\tau_g + 2n\pi\alpha) - \sin(n\Omega\tau_g)]. \tag{10c}$$

Mathematically, a very large number of harmonic terms should eliminate the Gibbs effect and virtually reconstruct the pulse-width modulated load. However, the amplitude drops at higher harmonics as evident by (10). We numerically (employing the Runge–Kutta routine) evaluate the effect of harmonic terms on nonlinear stick–slip response (with $\alpha = 0.8$, $\tau_g = 0$ at $\Omega = 0.45$). Virtually identical results are obtained with 50 or more harmonics. Consequently, 50 harmonic terms are utilized to approximate the pulse-width modulated normal load in this study. Further, for the sake of brevity, our research is primarily limited to the examination of the effect of duty ratio and therefore we assume zero time delay.

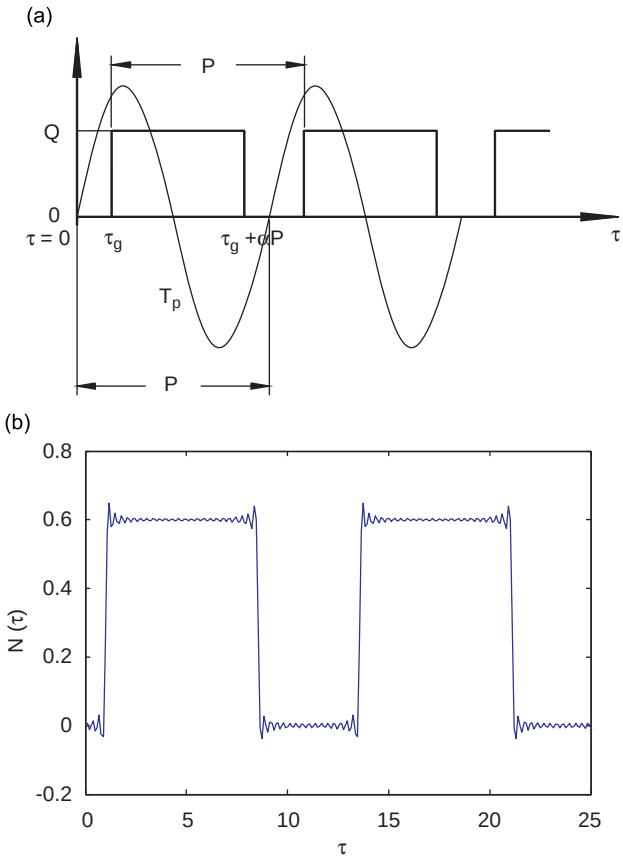

Fig. 3. A pulse width modulated normal load with duty ratio α and time delay τ_g: (a) schematic presentation; (b) reconstruction of the PWM normal load (at $\Omega = 0.5$) using 50 harmonic terms.

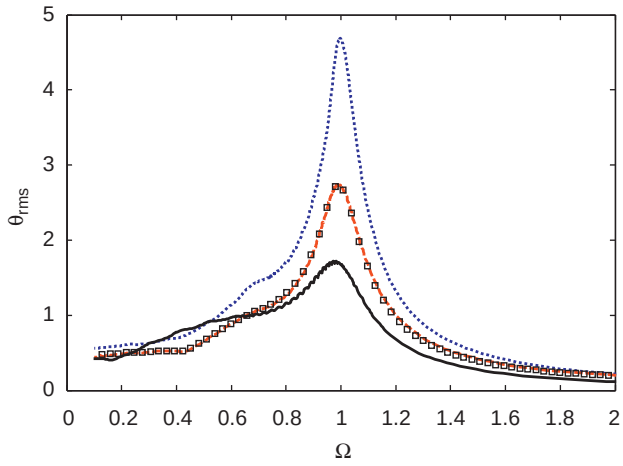

Fig. 4. Effect of pulse duty ratio α on the nonlinear frequency responses. Key: ●●●, $\alpha = 0.4$ using MHBM; − − −, $\alpha = 0.8$ using MHBM; —, $\alpha = 1.0$ using MHBM; □, $\alpha = 0.8$ using numerical integration with 50 harmonic terms.

5. Effect of duty ratio on nonlinear frequency responses

Fig. 4 shows the root-mean-square (rms) frequency responses when $\alpha = 0.4$, 0.8 and 1.0 (constant normal load). Again, the Runge–Kutta integration is employed to validate the nonlinear time-varying results obtained from MHBM when $\alpha = 0.8$. Observe that beyond the resonant frequency, the constant load ($\alpha = 1$) yields more vibration attenuation. From the corresponding time domain results, we know that the friction interface experiences pure slipping motion. Consequently,

a constant normal load certainly dissipates the maximum energy. On the other hand, we observe different, yet interesting, phenomenon at a lower frequency (below the resonance). As shown in Fig. 4, $\alpha = 0.4$ provides better vibration attenuation than $\alpha = 1.0$ from $\Omega = 0.31$ to 0.52,. This regime is even enhanced from $\Omega = 0.24$ to 0.65 when $\alpha = 0.8$. For example, at $\Omega = 0.45$, $\theta_{\mathrm{rms}}(\alpha = 1)/\theta_{\mathrm{rms}}(\alpha = 0.8) = 1.5$. This suggests that the employment of a constant normal load may not be the best vibration control strategy depending on the stick–slip regime. This phenomenon is attributed to the stick–slip motions. Analytically, the energy dissipation over one full period (P) is:

$$E_{\mathrm{dissipate}} = \int_0^P T_f(\theta', \tau)\theta' \, \mathrm{d}\tau. \tag{13}$$

The following two conditions should dissipate more energy under stick–slip: (1) The effective dissipation window, i.e. $T_f(\theta', \tau)\theta' \neq 0$ or $\theta'(\tau) \neq 0 \cap N(\tau) \neq 0$, should have a longer span within one period; (2) within that span, $\theta'(\tau)$ should have a higher value while Q remains fixed. Although $\alpha = 1$ provides a non-zero $N(\tau)$ during the whole period, the stick phase with $\theta' = 0$ consumes more time within one period. That implies that $E_{\mathrm{dissipate}}$, as defined by Eq. (13), may not achieve the maximum value. Consequently, $\alpha = 1$ does not necessarily provide more attenuation in certain frequency ranges.

To further examine the effects of α on frequency responses, a contour map of nonlinear responses $\theta_{\mathrm{rms}}(\alpha,\Omega)$ is generated as shown in Fig. 5. Both light (when $r\mu_s Q/T_p = 0.1$) and heavy load (when $r\mu_s Q/T_p = 0.6$) conditions are considered while recognizing that stick–slip motions tend to occur under a heavier load [4]. First, we note that a higher value of α reduces the vibration amplitude in the vicinity of primary resonance under both light and heavy loads, and the contour lines are dome-shaped accordingly. However, differences are found at off-resonant frequencies. Under the light load condition, we interestingly find that a change in α has minimal effect on the vibration amplitudes (as shown in Fig. 5a), except at lower frequencies where minor zig-zags indicate rather small effects.

In contrast, when the contour lines move away from the primary resonance regime under a heavy load as shown in Fig. 5b, zig-zag patterns are seen either below or above the resonance. Overall, $\alpha = 1$ still provides best attenuation beyond

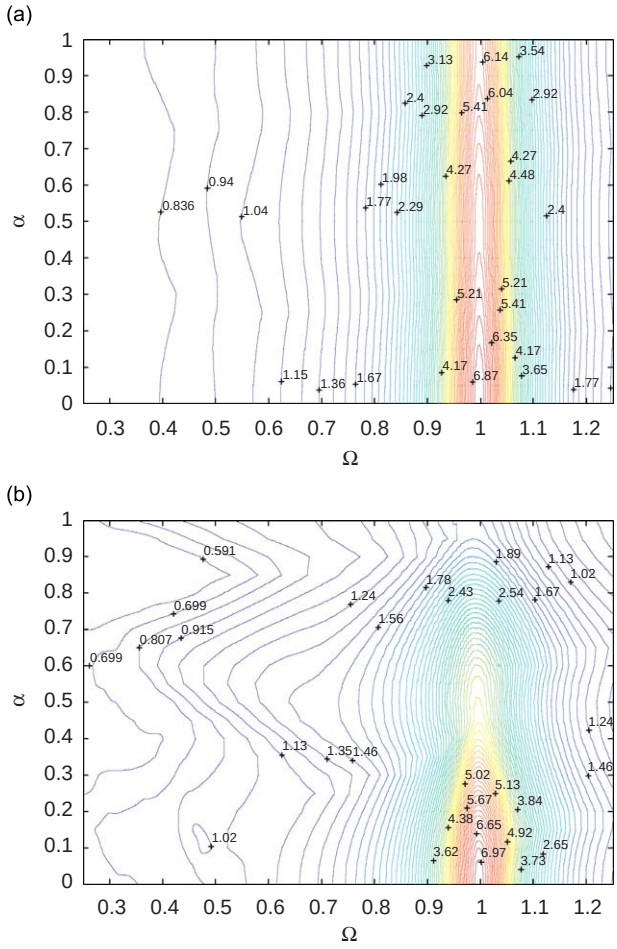

Fig. 5. Effect of duty ratio α on the nonlinear response map $\theta_{\mathrm{rms}}(\alpha,\Omega)$ with zero time delay ($\tau_g = 0$): (a) under the light load condition $r\mu_s Q/T_p = 0.1$; (b) under the heavy load condition $r\mu_s Q/T_p = 0.6$.

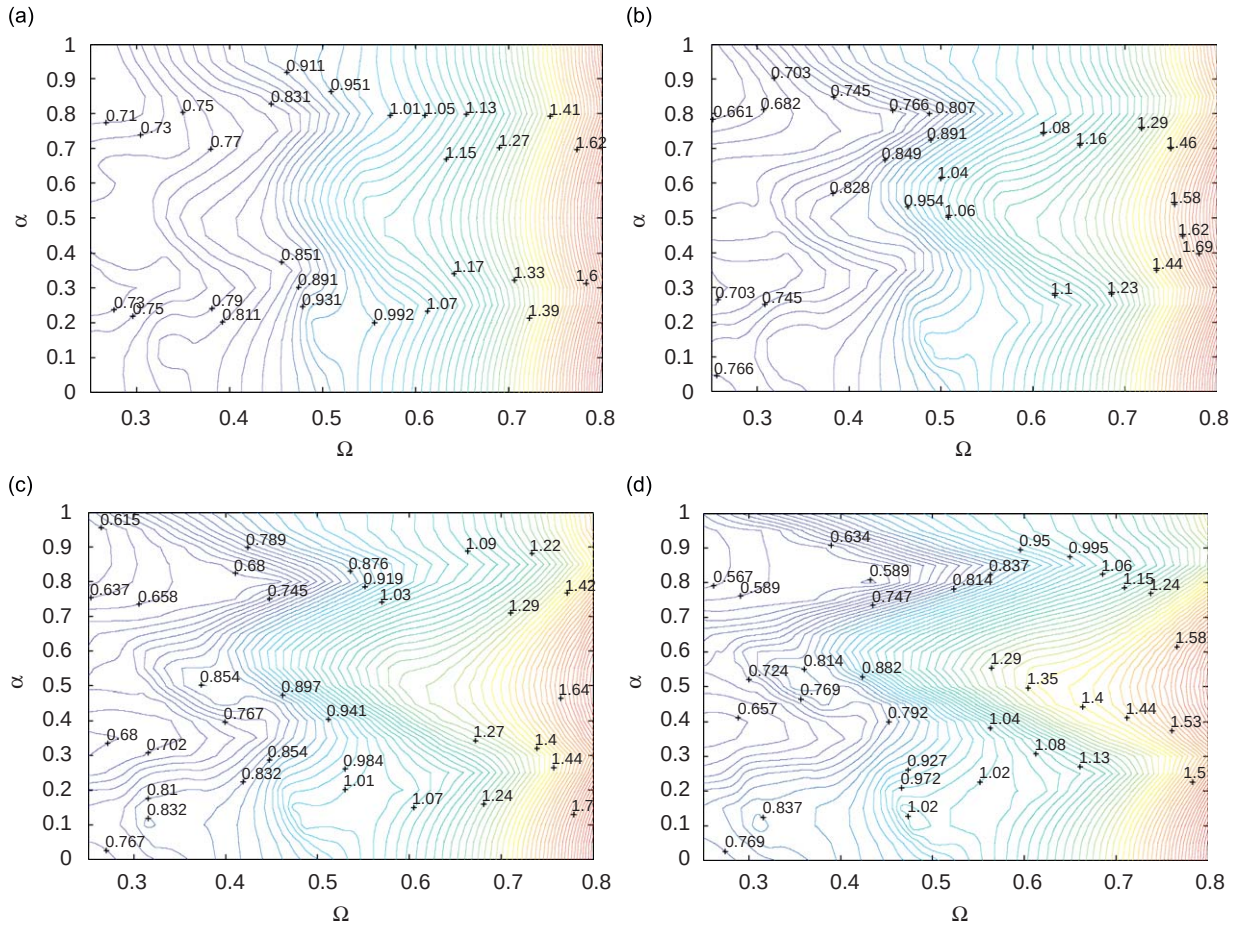

Fig. 6. Effect of duty ratio α on the nonlinear response map $\theta_{\mathrm{rms}}(\alpha,\Omega)$ with zero time delay: (a) $r\mu_s Q/T_p = 0.2$; (b) $r\mu_s Q/T_p = 0.3$; (c) $r\mu_s Q/T_p = 0.4$; and (d) $r\mu_s Q/T_p = 0.5$.

the resonance. Nonetheless, the contour lines are significantly "deformed" in the lower frequency regime as a result of significant stick–slip motions. When α is around 0.8, there exist an apparent regime where the contour curves bend deeply toward the higher frequency, which indicates the lowest vibration amplitudes at each excitation frequency. For example at $\Omega = 0.53$, $\theta_{\mathrm{rms}} = 0.591$ when $\alpha = 0.8$; this represents a 35% reduction in the vibration amplitude from $\alpha = 1$. Fig. 6 shows four additional sets of results with $r\mu_s Q/T_p = 0.2,\ 0.3,\ 0.4$ and 0.5, respectively. In all cases, the maximum vibration attenuation is found when α is around 0.8.

6. Conclusion

In this communication, forced vibration response characteristics of a single degree of freedom torsional system with combined Coulomb friction (under a periodically varying normal load) and viscous damping is studied. Two contributions emerge. First, an enhanced multi-term harmonic balance method has been successfully developed to construct the periodic solutions to a nonlinear time-varying system. Second, the effect of duty ratio of a pulse width modulated load is examined by assuming the classical Coulomb friction law. When the stick–slip motions occur, the system response depends on the duty ratio. Interestingly, a constant normal load may not be the best choice to suppress the vibration amplitude below the resonant frequency. Our investigations suggest that the most vibration attenuation is achieved when duty ratio is around 0.8; this should be examined further along with the effect of time delay. Future work will extend the enhanced semi-analytical method to multi-degree of freedom nonlinear systems with time-varying parameters or normal loads.

References

[1] J.P. Den Hartog, Forced vibrations with combined Coulomb and viscous friction, *Transaction of the ASME* APM-53-9 (1931) 107–115.
[2] T.K. Pratt, R. Williams, Nonlinear analysis of stick/slip motion, *Journal of Sound and Vibration* 74 (1981) 531–542.
[3] S.W. Shaw, On the dynamic response of a system with dry friction, *Journal of Sound and Vibration* 108 (1986) 305–325.

[4] C. Duan, R. Singh, Stick–slip behavior in torque converter clutch, *SAE Transactions, Journal of Passenger Car: Mechanical Systems* 116 (2005) 2785–2795.
[5] J. Kang, S. Choi, Brake dynamometer model predicting brake torque variation due to disc thickness variation, *Proceedings of the Institution of Mechanical Engineers, Part D: Journal of Automobile Engineering* 221(1) 49–55.
[6] C. Duan, R. Singh, Influence of harmonically-varying normal load on steady state behavior of a 2dof torsional system with dry friction, *Journal of Sound and Vibration* 294 (2006) 503–528.
[7] J. Badertscher, K.A. Cunefare, A.A. Ferri, Braking impact of normal dither signals, *Transactions of ASME, Journal of Vibration and Acoustics* 129 (2007) 17–23.
[8] C. Pierre, A.A. Ferri, E.H. Dowell, Multi-harmonic analysis of dry friction damped systems using an incremental harmonic balance method, *Transactions of ASME, Journal of Applied Mechanics* 52 (1985) 958–964.
[9] G. Von Groll, D.J. Ewins, The harmonic balance method with arc-length continuation in rotor/stator contact problems, *Journal of Sound and Vibration* 241 (2001) 223–233.
[10] T.C. Kim, T.E. Rook, R. Singh, Super-and sub-harmonic response calculations for a torsional system with clearance non-linearity using the harmonic balance method, *Journal of Sound and Vibration* 281 (2005) 965–993.
[11] C. Duan, R. Singh, Super-harmonics in a torsional system with dry friction path subject to harmonic excitation under a mean torque, *Journal of Sound and Vibration* 285 (2005) 803–834.
[12] C. Duan, R. Singh, Dynamics of a torsional system with harmonically varying dry friction torque, *Proceedings of 2007 International Symposium on Nonlinear Dynamics*, October Shanghai, 2007, pp. 1–6.
[13] J.R. Dormand, P.J. Prince, A family of embedded Runge–Kutta formulae, *Journal of Computational and Applied Mathematics* 6 (1980) 19–26.
[14] A. Kahraman, R. Singh, Non-linear dynamics of a spur gear pair, *Journal of Sound and Vibration* 142 (1990) 49–75.
[15] D.W. Jordan, P. Smith, *Non-linear Ordinary Differential Equations*, Oxford University Press, Oxford, 1999.